

SCALAR FIELD MODELS FOR DARK ENERGY

By

Hui-Yiing Chang

Dissertation

Submitted to the Faculty of the
Graduate School of Vanderbilt University
in partial fulfillment of the requirements

for the degree of

DOCTOR OF PHILOSOPHY

in

Physics

August, 2014

Nashville, Tennessee

Approved:

Robert J. Scherrer, Ph.D.

Thomas J. Weiler, Ph.D.

Andreas A. Berlind, Ph.D.

M. Shane Hutson, Ph.D.

John G. Ratcliffe, Ph.D.

DEDICATION

To my mother, Madam Soh Chiao-Yong, who made tremendous sacrifices which involved strains of the human spirit so that I can have the education, credentials and honors that she was deprived of as a result of prolonged communist oppression.

ACKNOWLEDGEMENTS

I am indebted to the generous financial support from the following sources which have enabled me to pursue studies and research that culminated in this dissertation: the National Science Foundation Graduate Research Fellowship under Grant No. DGE0946822, the Graduate Teaching Assistantship Award from the College of Arts and Sciences, the William and Nancy McMinn Graduate Fellowship Awards in Physics from the Endowed Funding, the Physics and Astronomy McMinn Fellowship from the College of Arts and Sciences, and the Scherrer Start Up Funds from the College of Arts and Sciences.

The following sources of financial support have allowed me to enrich this degree program by conducting research under mentors overseas: the National Science Foundation East Asia and Pacific Summer Institutes Fellowship and the Japan Society for the Promotion of Science, which sponsored my research program in Japan; the American Physical Society Indo-U.S. Science and Technology Forum Physics Student Visitation Program, which sponsored my research program in the Republic of India; the National Science Foundation East Asia and Pacific Summer Institutes Fellowship and the National Research Foundation of Korea, which sponsored my research program in the Republic of Korea; and the American Physical Society and the Sociedade Brasileira de Física Brazil-U.S. Physics Student Visitation Program, which sponsored my research program in the Federative Republic of Brazil.

I am especially grateful to my advisor, Dr. Robert Scherrer, who is also the Chair of the Physics and Astronomy Department, for his expert, systematic and kind mentorship in research as well as his professional guidance and repeated prompt assistance. In addition, I am deeply grateful to Dr. David Ernst, Professor of the Physics and Astronomy Department, for his altruistic continual valuable advisement and help in matters pertaining to my research and degree program. Also, Dr. Kelly Holley-Bockelmann, Associate Professor of the Physics and Astronomy Department, has to be acknowledged for mentoring me during my application for the National Science Foundation Graduate Research Fellowship. And, I am appreciative of Dr. Xiao Shen, Postdoctoral Fellow of the Physics and Astronomy Department, for resolving numerous problems with my computer system.

I would like to thank my mother, late father, maternal grandmother, godmother and paternal aunt, and my elder and younger sisters, who provided directly and indirectly various forms of support during the extensive period of my tertiary education. My present level of accomplishment would not have been possible without some of their support given sacrificially or unreservedly.

While I am geographically separated from my family, my pastor, the Rev. David Filson, and friends from my church have upheld me with the support and encouragement that I need, particularly through the challenging times of this degree program.

TABLE OF CONTENTS

DEDICATION..... ii

ACKNOWLEDGEMENTS iii

LIST OF FIGURES vi

Chapter

INTRODUCTION..... 1

1. COINCIDENCE PROBLEM IN CYCLIC PHANTOM MODELS OF THE UNIVERSE
..... **6**

1.1. Introduction6

1.2. The coincidence fraction in the cyclic phantom model.....8

1.3. Discussion14

2. INFLECTION POINT QUINTESSENCE 16

2.1. Introduction16

2.2. The inflection point quintessence model.....18

2.2.1. The cubic inflection point model.....19

2.2.2. Other inflection point models24

2.3. Conclusions27

3. A MODIFIED EXPONENTIAL POTENTIAL FOR QUINTESSENCE 29

3.1. Introduction29

3.2. Evolution of the scalar field30

3.3. Observational constraints	34
3.4. Discussion	37
REFERENCES	39

LIST OF FIGURES

1. The evolution of the scalar field ϕ as a function of time t for the potential $V(\phi) = V_0 + V_3\phi^3$, with $V_3/V_0 = 1$. Black (solid) curve is for $\phi_i = 1.76$; red (dashed) curve is for $\phi_i = 1.78$ 21

2. For the scalar field potential $V(\phi) = V_0 + V_3\phi^3$, the curves divide regions with different behaviors for ϕ as a function of the initial value of the field, ϕ_i , and the ratio of V_3 to V_0 . Above and to the right of the black (solid) curve, the field evolves through the inflection point at $\phi = 0$, while below and to the left of this curve, $\phi \rightarrow 0$ as $t \rightarrow \infty$. The regions below the green (dashed) and red (dotted) curves closely mimic Λ CDM. The region below the green curve has an equation of state parameter for ϕ satisfying $-1 < w < -0.95$ at all times up to the present, while the region below the red curve corresponds to $-1 < w < -0.9$ 22

3. The evolution of the scalar field equation of state w_ϕ as a function of the scale factor a , where $a = 1$ at the present. Blue (dotted) curve is for $\lambda = 10$; green (solid) curve is for $\lambda = 13$; red (dashed) curve is for $\lambda = 15$ 33

4. The evolution of the scalar field energy density parameter, Ω_ϕ , as a function of the scale factor a , where $a = 1$ at the present. Blue (dotted) curve is for $\lambda = 10$; green (solid) curve is for $\lambda = 13$; red (dashed) curve is for $\lambda = 15$ 34

INTRODUCTION

The expansion of the universe was discovered during the 1920's. Edwin Hubble was the first to notice a linear relationship between the velocities of distant galaxies receding from the earth and their distances from us, which is an evidence for the expansion of the universe. From charting the velocities of the galaxies against their distances, he discovered Hubble's law:

$$v = H_0 d, \quad (1)$$

where H_0 is now known as the Hubble constant, $v = zc$, z being the redshift of the light source, and d is the proper distance from the galaxy whose velocity is measured. The 0 subscript in the equation expresses that H_0 is the present-day value of H , the Hubble parameter.

The Friedmann equation gives the Hubble parameter as a function of the mean density of the universe. In a Friedmann–Robertson–Walker universe,

$$H^2 \equiv \left(\frac{\dot{a}}{a}\right)^2 = \frac{8\pi G}{3} \rho - \frac{K}{a^2}, \quad (2)$$

where a is the scale factor, G is the gravitational constant, ρ is the energy density, and K denotes the curvature of the universe. The dot indicates derivative with respect to time.

Observations indicate that $K \approx 0$, so we will assume a spatially-flat universe throughout. [1, 2]

Consider a barotropic fluid filling the universe. The equation of state (EoS) of this component is

$$w = p/\rho, \quad (3)$$

where p represents the pressure of the fluid. For example, matter has $w = 0$, and radiation has $w = 1/3$. Assume for now that w is constant. The time derivative of the Friedmann equation above is

$$\dot{H} = -4\pi G(p + \rho). \quad (4)$$

The continuity equation is

$$\dot{\rho} + 3H(p + \rho) = 0. \quad (5)$$

From the eqs. (2), (3) and (5), we derive

$$\rho(a) = \rho_0 a^{-3(1+w)}, \quad (6)$$

where ρ is the present-day energy density of the component that occupies the universe. Then

$$a \propto t^{2/3(1+w)}. \quad (7)$$

In a matter-dominated universe, $w = 0$, so $a \propto t^{2/3}$. In a radiation-dominated universe, $w = 1/3$, so $a \propto t^{1/2}$. In both cases, the expansion rate of the universe decelerates. [1, 2]

The accelerated expansion of the universe was discovered by the Supernova Cosmology Project headed by Saul Perlmutter and the High-Z Supernova Search Team led by Brian Schmidt and Adam Riess. Supernovae were used as standard candles for measuring cosmological distances. The Perlmutter project was started in 1988 to constrain cosmological parameters with the magnitude-redshift relation of Type Ia supernovae (SNe Ia). Methods were developed to study these supernovae at high redshift. By March 1998, more than 75 SNe Ia at redshift $z = 0.18 - 0.86$ were discovered and studied by the project. The study of 33 high-redshift SNe Ia resulted in a confidence region that indicated that the universe is expanding with an acceleration. Around the same time, work by Riess et al. (1998) arrived at the same conclusion.

[3] Specifically, for a flat cosmology, where

$$\Omega_M + \Omega_\Lambda = 1, \quad (8)$$

it was found that the density parameter of matter, $\Omega_M = 0.28^{+0.09}_{-0.08}$ (1σ statistical) $^{+0.05}_{-0.04}$ (identified systematics), and the data required a non-zero, positive cosmological constant Λ . [3] These

results were confirmed by the High-Z Supernova Search Team led by Adam Riess and Brian Schmidt.

From the Friedmann and \dot{H} equations, we have

$$\frac{\ddot{a}}{a} = -\frac{4\pi G}{3}(\rho + 3p). \quad (9)$$

In order for the expansion of the universe to accelerate, $\ddot{a} > 0$, resulting in $w < -1/3$. The component that is named to account for this acceleration is “dark energy”. [1] Ever since the discovery of the universe's accelerated expansion, there have been sundry proposed candidates for dark energy, which is one of the greatest unresolved mysteries in science today.

Einstein's cosmological constant Λ is a strong candidate for dark energy. He had originally introduced it in 1917 for a static universe, but retracted it after Hubble's discovery in 1929 of the expansion of the universe. [1] It was re-embraced by scientists when the universe was discovered to be expanding with an acceleration. The vacuum in the universe possesses an energy density, $\rho_\Lambda < 0$, that remains constant through time [4, 5], so $w = -1$. A model with cold dark matter (CDM) and a cosmological constant is called Λ CDM. For constant ρ , the Hubble rate H is also constant. From the Hubble equation, we derive $a = e^{Ht}$, which represents the de Sitter Universe. [1]

From the Friedmann equation, (2), the critical energy density ρ_c is found by assuming the universe to be flat, ie. $K = 0$ [6].

$$\rho_c = \frac{3H^2}{8\pi G} \quad (10)$$

Therefore, the present-day critical density is

$$\rho_{c0} = \frac{3H_0^2}{8\pi G}. \quad (11)$$

The present-day density parameter of each component that the universe comprises is

$\Omega_{x0} = \rho_{x0}/\rho_{c0}$, where x represents the particular component. [1] Considering the possible components of the universe, for one that comprises radiation, matter and the cosmological constant, the total energy density is

$$\rho = \rho_\gamma + \rho_M + \rho_\Lambda = \rho_{\gamma0}a^{-4} + \rho_{M0}a^{-3} + \rho_{\Lambda0}. \quad (12)$$

However, there remain distinct unresolved issues with the Λ CDM model, one major one being the cosmological constant problem. According to observations, $\Lambda \approx H_0^2$. From that, we derive the energy density, $\rho_\Lambda \approx 10^{-47} \text{ GeV}^4$. However, the vacuum energy density computed by summing the zero-point energies, $\rho_{vac} \approx 10^{74} \text{ GeV}^4$, which is 121 orders of magnitude greater than the observed value. [1, 4] Another unresolved issue is the coincidence problem. The matter energy density far exceeded the dark energy density in the distant past. The former decreases with time while the latter is constant, such that dark energy density will far exceed matter energy density in the distant future. It appears a coincidence that we are existing during an epoch when the energy densities of both components are comparable.

As scientists, since we entertain all possibilities related to a particular issue, we consider dark energy with a dynamical w , meaning one that changes through time. Quintessence models of the universe which contain a scalar field ϕ , hypothesized to be time-varying dark energy, have been proposed. [1]

There are alternative scalar field models that have been proposed to accommodate observations. In the k -essence cosmology, modifications to the standard kinetic energy of the scalar field results in the universe's accelerated expansion. In another model, a rolling tachyon

field has an EoS that repeatedly reaches -1 , causing inflation at high energy. The phantom cosmology for dark energy will be explained in the next section. [1]

Chapter 1 of this dissertation deals with the coincidence problem. It is ameliorated within an alternative model of the universe, the Cyclic Phantom Model. This chapter has been published in Physical Review D [7].

Chapter 2 examines Inflection Point Quintessence, a model we have developed for a dynamical scalar field that rolls near an inflection point in its potential. This model is found to be a satisfactory model for dark energy. This chapter has been published as a paper in Physical Review D [8].

Chapter 3 examines another quintessence model for dark energy, namely the sum of an exponential potential and a constant potential. This model has significant energy density at early times, mimicking “extra” neutrinos.

The cosmologies explored in all three chapters contain scalar fields. I hope that these three cosmologies presented in my dissertation will further the revelation of dark energy by providing ideas for more accurate models of the universe.

CHAPTER 1

COINCIDENCE PROBLEM IN CYCLIC PHANTOM MODELS OF THE UNIVERSE

1.1 Introduction

Cosmological data [9–12] indicate that approximately 70% of the energy density in the universe is in the form of an exotic, negative–pressure component, called dark energy, with roughly 30% in the form of nonrelativistic matter (including both baryons and dark matter). The dark energy component can be parametrized by its equation of state parameter, w , defined as the ratio of the dark energy pressure to its density:

$$w = p_{DE} / \rho_{DE}, \quad (13)$$

where $w = -1$ corresponds to a cosmological constant. For constant w , the energy density of the dark energy, ρ_{DE} , scales as

$$\rho_{DE} = \rho_{DE0} \left(\frac{R}{R_0} \right)^{-3(1+w)}, \quad (14)$$

where R is the scale factor, and ρ_{DE0} and R_0 are the density and scale factor, respectively, at the present. (We will use zero subscripts throughout to refer to present–day values). Observations constrain w to be very close to -1 . For example, if w is assumed to be constant, then $-1.1 \lesssim w \lesssim -0.9$ [13, 14]. Thus, the dark energy density varies relatively slowly with scale factor.

The matter density, in contrast, scales as

$$\rho_M = \rho_{M0} \left(\frac{R}{R_0} \right)^{-3} \quad (15)$$

This leads to the well–known coincidence problem: while the matter and dark energy densities today are nearly within a factor of two of each other, at early times $\rho_M \gg \rho_{DE}$, and in the far

future we expect $\rho_{DE} \gg \rho_M$. It would appear, then, that we live in a very special time: this is the coincidence problem.

While it is possible that this coincidence has no deeper explanation, numerous solutions have been proposed to explain it. In the k -essence model of Armendariz-Picon et al. [15], the dark energy density tracks the radiation density during the radiation-dominated epoch but approaches a constant value during the matter-dominated epoch. Another proposed solution is a universe which experiences an alternation of matter domination and dark energy domination, either through a scalar field with oscillatory behavior [16, 17], or as a result of a variety of scalar fields with a wide range of energy densities [18]. Another possible solution for the coincidence problem is a coupling of the matter and quintessence fields so that energy is transferred between them [19, 20]. Garriga and Vilenkin [21] proposed an anthropic solution to the coincidence problem. Scherrer [22] suggested that the coincidence problem could be resolved in the context of phantom dark energy models. In such models, the universe terminates in a singularity at a finite time [23, 24], so that the fraction of time for which the dark energy and matter densities are relatively close can be a significant fraction of the universe's (finite) lifetime. Other models in which the coincidence problem is resolved by the universe having a finite lifetime were examined by Barreira and Avelino [25]. Lineweaver and Egan [26, 27] have proposed that the coincidence is related to the formation rate for habitable planets.

Here we examine another plausible solution to the coincidence problem, in the context of cyclic phantom models, of the type proposed by Ilie et al. [28]. In these models, the universe goes through repeated cycles of matter/radiation domination followed by a dark energy/inflationary phase. Ilie et al. indicated that their model cannot address the coincidence problem, but we show here that it provides an elegant resolution of this problem. Within each

cycle, there is a significant period in which the dark energy and matter densities are comparable. Since these cycles repeat endlessly, it is not surprising that we find ourselves in an epoch in which the dark energy and matter densities are of the same order of magnitude. Similar models have been proposed by Creminelli et al. [29] and by Xiong et al. [30].

We make this argument quantitative in the next section. Rather than confining ourselves to the specific model of Ref. [28], we use a toy model which captures the essential features of a generic cyclic phantom model. We also derive a useful approximation to the coincidence fraction in the limit where w is close to -1 (as observations require). Our results are discussed in Sec. 1.3.

1.2 The coincidence fraction in the cyclic phantom model

In the cyclic phantom model proposed by Ilie et al. [28], the universe contains radiation, a scalar field, and a hidden matter sector. Inflationary expansion is followed by a reheating phase, during which radiation becomes the dominant component. Eventually the scalar field and hidden matter densities both track the radiation density but are subdominant. At late times, the hidden matter and scalar field begin to behave as a phantom field with $w < -1$, and the universe undergoes superaccelerated expansion. This phase then transitions to de Sitter inflation, and the cycle repeats itself.

Much of the complexity of the model discussed in Ref. [28] stems from the need to have a plausible mechanism for the universe to transition from one phase of the expansion to the next. Since we are primarily interested in the behavior of the scale factor as a function of time, we will consider a toy model that approximates the general behavior of a cyclic phantom model. (This is also necessitated by the fact that the model introduced in Ref. [28] does not contain a matter

component). The use of such a toy model has the additional advantage of being applicable to more general cyclic phantom models than the specific model in Ref. [28] (As we have already noted, a number of similar models have been proposed [29, 30].)

In our toy model, the universe undergoes an initial “standard” expansion, consisting of a radiation–dominated era, followed by a matter–dominated era. An additional dark energy component is present, which tracks the matter or radiation density, but which is subdominant (so that $\rho_{DE} \ll \rho_M$ in the matter–dominated era). When the dark energy density reaches some lower energy scale m (so that $\rho_{DE} \sim m^4$), the dark energy assumes a phantom behavior, with equation of state parameter $w < -1$, and the universe undergoes superaccelerated expansion. This phantom phase terminates when the dark energy density (which is increasing with the expansion) reaches some upper energy scale M , so that $\rho_{DE} \sim M^4$. The universe then enters a de Sitter phase, which ends with reheating and a return to the radiation–dominated era.

The solution to the coincidence problem in this model arises because the universe naturally spends a significant fraction of the time in a state in which the densities of the dark energy and the matter are of the same order of magnitude. Conceptually, then, this solution resembles that of Dodelson et al. [16], in which the ratio of dark energy density to the density of the matter/radiation component oscillates with time. Mathematically, however, it more closely resembles the discussion in Ref. [22] for models with a single phantom phase terminating in a big rip, and it is this latter approach which we will follow in analyzing the cyclic phantom model.

Our goal is to derive the fraction of the time that the universe spends in a coincidental state, defined to be a state for which the ratio of the density of dark energy to the density of

matter lies within some fixed range close to 1. More specifically, let ρ_{DE} be the dark energy density, and ρ_M be the nonrelativistic matter density, and define the ratio r as in Ref. [22]:

$$r = \frac{\rho_{DE}}{\rho_M}. \quad (16)$$

We will then define a coincidental state to be one for which r lies in the range

$$r_1 < r < r_2, \quad (17)$$

where the values for r_1 and r_2 that define a ‘‘coincidence’’ are, of course, somewhat arbitrary.

We assume a flat Friedman–Robertson–Walker model, so that the evolution of the scale factor is given by

$$\left(\frac{\dot{R}}{R}\right)^2 = \frac{8}{3}\pi G\rho. \quad (18)$$

At late times, the expansion of the universe is dominated by matter and dark energy. To simplify matters, we assume throughout that w is constant. Then we can use Eqs. (14) and (15) to give

$$\left(\frac{\dot{R}}{R}\right)^2 = \frac{8}{3}\pi G \left[\rho_{M0} \left(\frac{R}{R_0}\right)^{-3} + \rho_{DE0} \left(\frac{R}{R_0}\right)^{-3(1+w)} \right]. \quad (19)$$

The time the universe takes in expanding from scale factor R_1 to R_2 is

$$t_{12} = \int_{R_1}^{R_2} R^{-1} \left\{ \frac{8}{3}\pi G \left[\rho_{M0} \left(\frac{R}{R_0}\right)^{-3} + \rho_{DE0} \left(\frac{R}{R_0}\right)^{-3(1+w)} \right] \right\}^{\frac{1}{2}} dR, \quad (20)$$

and the time the universe takes to complete one cycle is

$$t_{cycle} = \int_{R=0}^{R=R_{max}} R^{-1} \left\{ \frac{8}{3}\pi G \left[\rho_{M0} \left(\frac{R}{R_0}\right)^{-3} + \rho_{DE0} \left(\frac{R}{R_0}\right)^{-3(1+w)} \right] \right\}^{\frac{1}{2}} dR, \quad (21)$$

where R_{max} is the scale factor at which the dark energy density reaches its maximum value of M^4 and the de Sitter phase begins. Note that the integrand in equation (21) is valid only after the dark energy begins to behave as a phantom, but the error involved in extrapolating it back to $R=0$ is negligible.

The fraction of time in each cycle that the universe spends in expanding from R_1 to R_2 is $f = t_{12}/t_{cycle}$. As in Ref. [22], we can rewrite t_{12} and t_{cycle} in terms of r . Taking r_1 to be the value of r at the beginning of the period of coincidence and r_2 as that at the end, the fraction of time in each cycle that the universe spends in a coincidental state is

$$f = \frac{\int_{r_1}^{r_2} r^{-\frac{2w+1}{2w}} / \sqrt{1+r} dr}{\int_0^{r=M^4/\rho_{M_{max}}} r^{-\frac{2w+1}{2w}} / \sqrt{1+r} dr}, \quad (22)$$

where $\rho_{M_{max}}$ is the value of the matter density at R_{max} . Since the cycles are identical and repeat indefinitely, f is also the fraction of the entire universe's lifetime that is spent in a coincidental state.

This coincidence fraction is at least as large as in the case of a future big rip singularity [22], and in principle it can be even larger, since the upper limit in the denominator of equation (22) is finite in the case considered here. This upper limit is enormous, but the integral converges very slowly for w near -1 , so it is useful to see how small M^4 needs to be in order for the result to diverge significantly from the case investigated in Ref. [22]. We have

$$\rho_{DE0} \left(\frac{R_{max}}{R_0} \right)^{-3(1+w)} = M^4. \quad (23)$$

Therefore, the matter density at R_{max} can be expressed as

$$\rho_{M_{max}} = \rho_{M0} \left(\frac{R_{max}}{R_0} \right)^{-3} = \rho_{M0} \left(\frac{M^4}{\rho_{DE0}} \right)^{\frac{1}{1+w}} \quad (24)$$

This allows us to express the upper limit of integration in the denominator of Eq. (22) as

$$r = \frac{M^4}{\rho_{M_{max}}} = \left(\frac{\rho_{DE0}}{\rho_{M0}} \right) \left(\frac{M^4}{\rho_{DE0}} \right)^{\frac{w}{1+w}}. \quad (25)$$

At the present, we have $\rho_{M0} \sim \rho_{DE0}$. Using this in Eq. (25), we can rewrite Eq. (22) as

$$f = \frac{\int_{r_1}^{r_2} r^{-\frac{2w+1}{2w}} / \sqrt{1+r} dr}{\int_0^{r=(M/E_{DE0})^{4w/(1+w)}} r^{-\frac{2w+1}{2w}} / \sqrt{1+r} dr}, \quad (26)$$

where the present-day energy scale of the dark energy is $E_{DE0} \sim 10^{-3}$ eV, and $\rho_{DE0} = E_{DE0}^4$.

The denominator in Eq. (26) can be expressed as

$$\begin{aligned} \int_0^{r=(M/E_{DE0})^{4w/(1+w)}} r^{-\frac{2w+1}{2w}} / \sqrt{1+r} dr &= \int_0^\infty r^{-\frac{2w+1}{2w}} / \sqrt{1+r} dr - \int_{r=(M/E_{DE0})^{4w/(1+w)}}^\infty r^{-\frac{2w+1}{2w}} / \sqrt{1+r} dr \\ &\approx \frac{\Gamma\left(-\frac{1}{2w}\right)\Gamma\left(\frac{1}{2} + \frac{1}{2w}\right)}{\Gamma\left(\frac{1}{2}\right)} - \frac{2w}{1+w} \left(\frac{M}{E_{DE0}} \right)^{-2}, \end{aligned} \quad (27)$$

where we have used the fact that $M/E_{DE0} \gg 1$ to simplify the second term on the right-hand

side.

We now use the constraint that observations require w to be close to -1 . (Note that we do not take $w = -1$, as this would imply $M^4 = \rho_{DE0}$ and invalidate the entire model. However, a value of w even slightly less than -1 allows for a phantom model with $M^4 \gg \rho_{DE0}$.) In the limit where $w \rightarrow -1$, the numerator in Eq. (26) can be approximated as

$$\int_{r_1}^{r_2} \frac{r^{-\frac{2w+1}{2w}}}{\sqrt{1+r}} dr \approx 2 \ln \frac{\sqrt{r_2} + \sqrt{1+r_2}}{\sqrt{r_1} + \sqrt{1+r_1}}. \quad (28)$$

Further, we can simplify Eq. (27) in the limit where w is close to -1 (note that $\Gamma(z) \sim 1/z$ as $z \rightarrow 0$), to give

$$\int_0^{r=(M/E_{DE0})^{4w/(1+w)}} \frac{r^{-\frac{2w+1}{2w}}}{\sqrt{1+r}} dr \approx \frac{-2}{1+w} \left[1 - \left(\frac{M}{E_{DE0}} \right)^{-2} \right], \quad (29)$$

and our final expression for the coincidence fraction becomes

$$f \approx -(1+w) \ln \frac{\sqrt{r_2} + \sqrt{1+r_2}}{\sqrt{r_1} + \sqrt{1+r_1}} \bigg/ \left[1 - \left(\frac{M}{E_{DE0}} \right)^{-2} \right]. \quad (30)$$

The corresponding expression for the case of a phantom model with a future singularity is identical to Eq. (30) without the $(M/E_{DE0})^{-2}$ in the denominator. This difference is negligible as long as $M \gg E_{DE0}$, as it must be in any reasonable cyclic phantom model. This is just another way of saying that the time needed for the universe to expand from the energy scale M to a future singularity is negligible compared to the time for the expansion up to M . Thus, the value for f in the cyclic phantom models is nearly identical to its value in models with a future singularity, and both are given (for w close to -1) by

$$f \approx -(1+w) \ln \frac{\sqrt{r_2} + \sqrt{1+r_2}}{\sqrt{r_1} + \sqrt{1+r_1}}. \quad (31)$$

Equation (31) is our main result.

As noted in Ref. [22], the exact values of r_1 and r_2 are not well-defined, since the definition of a coincidence is somewhat arbitrary. However, if we require, for example, that the dark energy and dark matter densities be within an order of magnitude of each other, then

$r_1 = 1/10$ and $r_2 = 10$, yielding $f = -1.56(1+w)$. In this case, a coincidence fraction as large as $f = 0.1$ can be obtained for $w = -1.06$. Thus, even for w quite close to -1 , the oscillating phantom model provides a solution to the coincidence problem.

1.3 Discussion

The cyclic phantom model provides an attractive solution to the coincidence problem, since the universe spends an appreciable fraction, f , of each cycle in a state for which the dark energy and matter densities are of the same order of magnitude. For the models considered here, we have shown that this fraction is essentially identical to the corresponding fraction in phantom models with a big rip. However, the cyclic phantom model provides a more credible solution to the coincidence problem, in the sense that it does not entail a future singularity. The cyclic phantom model has the further advantage of unifying inflation and dark energy. (Indeed, that was the original motivation for this model.) Although we have analyzed a generic toy model, these results apply, for example, to the model discussed in Ref. [28], as long as this model is modified to include a matter component with the appropriate density. In Ref. [28], the upper and lower energy scales were taken to be $m \sim 1$ meV and $M \sim 10^{15}$ GeV, but as we have shown, the value for f is actually independent of m and M as long as $M \gg E_{DE0}$.

In the observationally allowed limit where $|1+w| \ll 1$, the coincidence fraction f is $-(1+w)$ times a constant of order unity. Current constraints on w allow for a nonnegligible value for f . However, if future observations force $1+w$ to be sufficiently close to zero, this scenario for resolving the coincidence problem (along with that outlined in Ref. [22]) will be

ruled out. Of course, these results assume a constant value for w . If one assumes a time-varying w , then the value for f can be larger than in constant w models [31].

CHAPTER 2

INFLECTION POINT QUINTESSENCE

2.1 Introduction

While a model with a cosmological constant and cold dark matter (Λ CDM) is consistent with current observations, there are many realistic models of the universe that have a dynamical equation of state. For example, one can consider quintessence models, with a time-dependent scalar field, ϕ , having potential $V(\phi)$ [36–39]. (See Ref. [1] for a review.)

In order to produce a present-day value of w close to -1 , we require $p \approx -\rho$, so that $\dot{\phi}^2 \ll V(\phi)$ at present. One way to achieve this is for ϕ to be located in a very flat portion of the potential, so that

$$\left(\frac{1}{V} \frac{dV}{d\phi}\right)^2 \ll 1. \quad (32)$$

Several previous papers have investigated such models in which equation (32) is satisfied when the potential is close to linear [40, 41] or close to a local maximum [42] or minimum [43].

Here we examine the next higher-order extension of this idea: quintessence with a scalar field evolving near an inflection point of the potential. Scalar field models with an inflection point in the potential have been investigated previously in connection with inflation [44–58] and have been dubbed “inflection point inflation”. The major difference between these inflation models and the inflection point quintessence models we examine here is that inflation takes place in a scalar-field-dominated universe, while for the case of dark energy, we are interested in the evolution of the quintessence field at low redshift, when the Friedman equation must include

both the scalar field and nonrelativistic matter. Thus, results from inflection point models for inflation will not necessarily carry over into inflection point quintessence.

In investigating the evolution of inflection point quintessence, there are two important questions to address. The first is whether the scalar field rolls slowly enough near the inflection point to generate the observed value of w near -1 , for consistency with the observations. The second issue is whether ϕ evolves to a constant value at the inflection point, generating a model for which $w \rightarrow -1$ asymptotically, and yielding a model essentially indistinguishable from a cosmological constant, or whether ϕ rolls through the inflection point, so that w deviates away from -1 eventually. The latter possibility would produce a transient stage of acceleration, rather than an asymptotic de Sitter evolution. This is of interest because an eternally accelerating universe presents a problem for string theory, inasmuch as the S-matrix in this case is ill-defined [59, 60]. Consequently, some effort has gone into the development of models in which the observed acceleration is a transient phenomenon [61–70]. Our model represents another example of this sort of transient acceleration for the case in which ϕ evolves through the inflection point.

In the next section, we present the general models under discussion. Unlike the linear and quadratic potentials examined in Refs. [40–43], the simplest version of inflection point quintessence, with a cubic term in the potential, does not yield a simple analytic expression for the evolution, so we solve it numerically in Sec. 2.2.1 and determine the regions in parameter space for which the model produces transient or eternal acceleration. We also determine the range of parameters for which $w \approx -1$ at all times up to the present. In Sec. 2.2.2, we examine other inflection point models, demonstrating that some of these do have analytic descriptions for their behavior. Our conclusions are summarized in Sec. 2.3.

2.2 The inflection point quintessence model

We assume that the dark energy is given by a minimally coupled scalar field, with equation of motion

$$\ddot{\phi} + 3H\dot{\phi} + \frac{dV}{d\phi} = 0, \quad (33)$$

where the dot indicates the derivative with respect to time, and H is the Hubble parameter, given by

$$H^2 = \left(\frac{\dot{a}}{a}\right)^2 = \frac{\rho_\phi + \rho_M}{3}, \quad (34)$$

where we assume a flat universe and consider only times sufficiently late that the expansion is dominated by matter and dark energy. (We take $\hbar = c = 8\pi G = 1$ throughout.) In Eq. (34), the scalar field energy density is

$$\rho_\phi = \frac{1}{2}\dot{\phi}^2 + V(\phi), \quad (35)$$

and the matter energy density is

$$\rho_M = \rho_{M0}a^{-3}. \quad (36)$$

The scalar field pressure is

$$p_\phi = \frac{1}{2}\dot{\phi}^2 - V(\phi), \quad (37)$$

and the equation of state parameter, w , is given by Eq. (13).

We will consider the general case of potentials with an inflection point in the potential.

The simplest example of such a model is a potential of the form

$$V(\phi) = V_0 + V_3(\phi - \phi_0)^3, \quad (38)$$

which has an inflection point with $dV/d\phi = 0$ at $\phi = \phi_0$. This is the potential that we will investigate in the next section. It is not only the simplest inflection point quintessence model, but as we shall see, it also produces some of the most interesting behavior.

The potential in Eq. (38) can be generalized in several ways. For instance, one can add linear and quadratic terms to obtain

$$V(\phi) = V_0 + V_1(\phi - \phi_0) + V_2(\phi - \phi_0)^2 + V_3(\phi - \phi_0)^3. \quad (39)$$

It is also possible to consider more general inflection points produced by models with other powers of ϕ in the potential, i.e., potentials of the form

$$V(\phi) = V_0 + V_n(\phi - \phi_0)^n. \quad (40)$$

We will examine the models given by Eqs. (39)–(40) in Sec. 2.2.2.

Since we are interested in the behavior of the scalar field near the inflection point, we will take Eqs. (38)–(40) to refer only to the behavior of $V(\phi)$ in the region near the inflection point and make no assumptions about what the rest of the potential looks like. Thus, our results will be more general than if we had assumed that these were the exact forms for the potential for all values of ϕ . Furthermore, the fact that these potentials are not bounded from below as $\phi \rightarrow -\infty$ is not pathological, since we do not assume that Eqs. (38)–(40) apply in this limit.

2.2.1 The cubic inflection point model

Consider first the potential given by Eq. (38). Equation (33) becomes

$$\ddot{\phi} + 3H\dot{\phi} + 3V_3(\phi - \phi_0)^2 = 0. \quad (41)$$

The evolution of ϕ is specified by four parameters, namely the initial values of ϕ and $\dot{\phi}$, and the values of V_0 and V_3 . However, some simplifications are possible.

We first note that the value of ϕ_0 has no effect on any physically observable quantities, so we can redefine the field to take $\phi_0 = 0$, and equation (41) becomes

$$\ddot{\phi} + 3H\dot{\phi} + 3V_3\phi^2 = 0, \quad (42)$$

with H given by

$$H^2 = \frac{1}{3} \left(\rho_{M0} a^{-3} + \frac{1}{2} \dot{\phi}^2 + V_0 + V_3 \phi^3 \right). \quad (43)$$

In order for the models examined here to be consistent with current observations, they must closely resemble Λ CDM, which is possible only if V_0 corresponds to the observed present-day dark energy density. Having fixed V_0 , we can completely specify the models by the value of V_3/V_0 . We will further assume for simplicity that $\dot{\phi}_i = 0$, i.e., the field is initially at rest. For many models of interest the damping term in Eq. (33) will tend to drive $\dot{\phi}$ to 0 at early times, giving the initial condition we consider here.

Hence, we are left with a model that is completely specified by V_3/V_0 and by the initial value of the scalar field, ϕ_i . We have numerically integrated Eqs. (42) and (43) to determine the behavior of $\phi(t)$ as a function of V_3/V_0 and ϕ_i . We find two distinct possible behaviors for ϕ : the field can either evolve past the inflection point at $\phi = 0$, or else it can evolve smoothly to $\phi = 0$ as $t \rightarrow \infty$. These two different types of behavior are shown in Fig. 1. The two $\phi(t)$ trajectories in this figure both have $V_3/V_0 = 1$, but slightly different initial values of ϕ , resulting in nearly identical evolution until the field approaches the inflection point, where the trajectories diverge to give very different asymptotic behaviors.

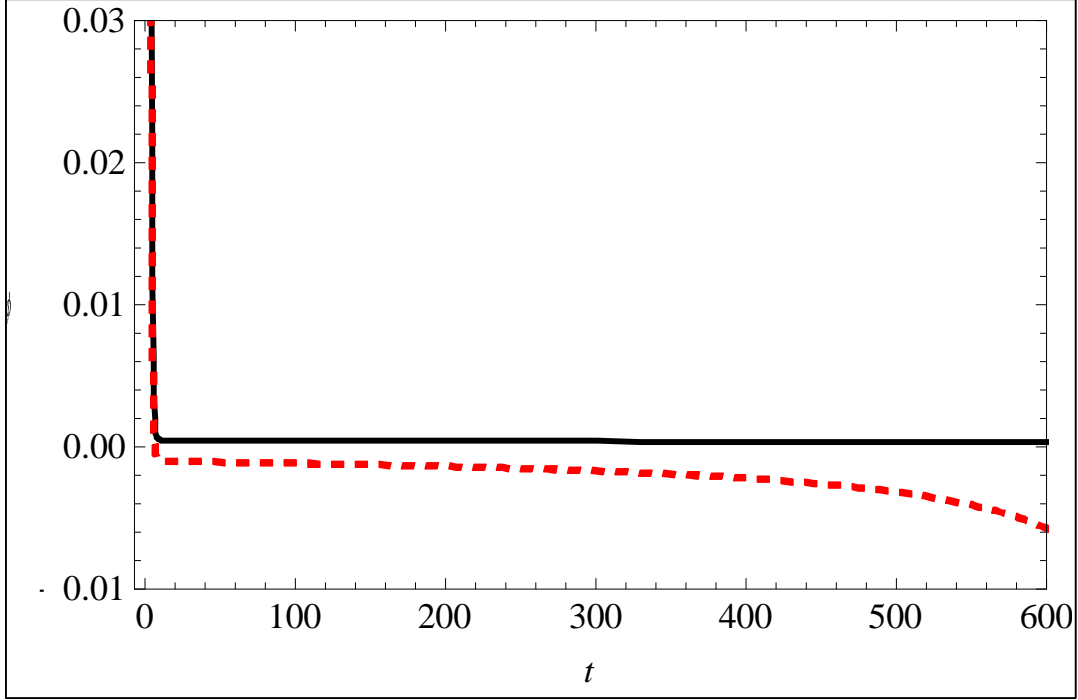


Fig. 1. The evolution of the scalar field ϕ as a function of time t for the potential $V(\phi) = V_0 + V_3\phi^3$, with $V_3/V_0 = 1$. Black (solid) curve is for $\phi_i = 1.76$; red (dashed) curve is for $\phi_i = 1.78$.

We find that for fixed ϕ_i , a sufficiently large value of V_3/V_0 causes the scalar field to evolve through the inflection point, while for smaller values of V_3/V_0 the field evolves asymptotically to $\phi = 0$ as $t \rightarrow \infty$. This is illustrated in Fig. 2. The region above the black (solid) curve gives a field that evolves through the inflection point, while the region below this curve has $\phi \rightarrow 0$ as $t \rightarrow \infty$. Note, however, that for sufficiently small values of V_3/V_0 , the field never transitions through the inflection point for any value of ϕ_i so the black curve becomes a horizontal line for large ϕ_i . We can define a critical value, $(V_3/V_0)_c$, below which evolution through the inflection point becomes impossible. Our numerical results indicate that $0.77 < (V_3/V_0)_c < 0.78$.

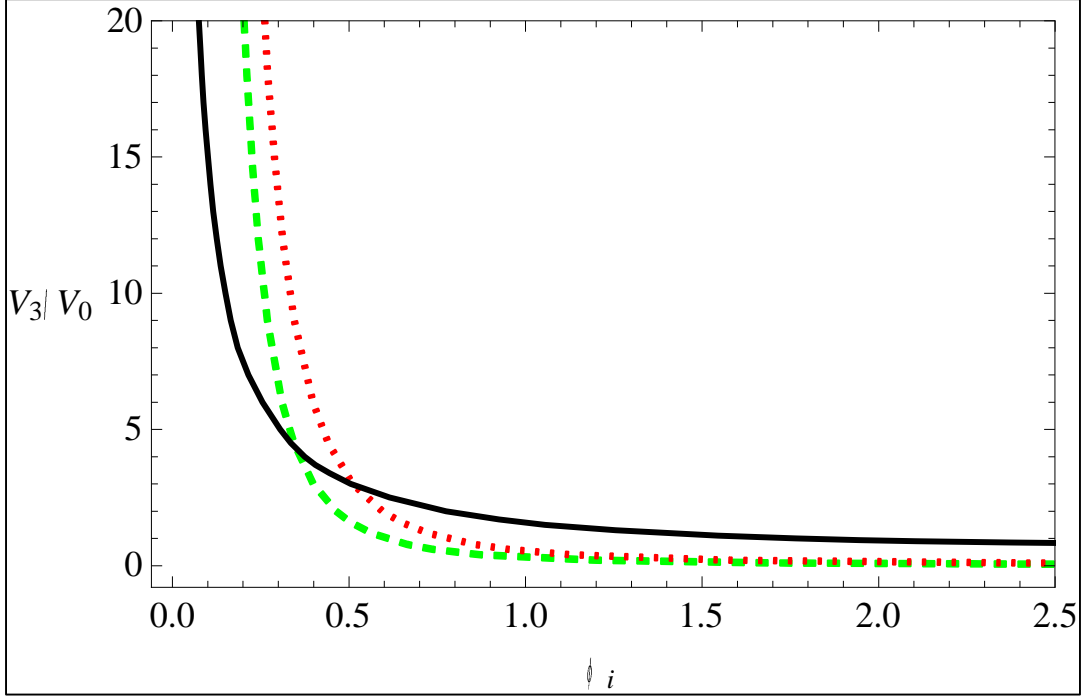


Fig. 2. For the scalar field potential $V(\phi) = V_0 + V_3\phi^3$, the curves divide regions with different behaviors for ϕ as a function of the initial value of the field, ϕ_i , and the ratio of V_3 to V_0 . Above and to the right of the black (solid) curve, the field evolves through the inflection point at $\phi = 0$, while below and to the left of this curve, $\phi \rightarrow 0$ as $t \rightarrow \infty$. The regions below the green (dashed) and red (dotted) curves closely mimic Λ CDM. The region below the green curve has an equation of state parameter for ϕ satisfying $-1 < w < -0.95$ at all times up to the present, while the region below the red curve corresponds to $-1 < w < -0.9$.

Note that a similar study was undertaken by Itzhaki and Kovetz [52], who explored the asymptotic evolution of the scalar field in inflection point inflation. Their study differs from ours in that we include nonrelativistic matter, which alters the evolution of H in equation (42). However, we find that matter is subdominant as $\phi \rightarrow 0$ for the model parameters lying along the transition regime defined by the black curve in Fig. 2. Hence, we would expect our results to agree with Ref. [52] with regard to the existence of a critical value of V_3/V_0 below which the field can never cross the inflection point, and Itzhaki and Kovetz do, indeed, observe such

behavior. They find $(V_3/V_0)_c = 0.7744$, in agreement with our results for the quintessence model.

The results displayed in Figs. 1–2 show that the inflection point quintessence model can lead to two very different future evolutionary paths for the universe. When ϕ asymptotically goes to zero, we are left with a model essentially identical to Λ CDM, with a de Sitter evolution. However, the second possibility, in which ϕ evolves through the inflection point, yields a model in which the accelerated expansion of the universe is a transient phenomenon. As noted earlier, we make no assumptions about $V(\phi)$ far from the inflection point, so the future evolution of the universe in this case will depend on the particular form for $V(\phi)$ with $\phi < 0$.

Clearly the first possibility can be made consistent with the observations, since the current observational data is well-fit by Λ CDM. A more interesting question is whether the models with transient acceleration, in which ϕ passes through the inflection point, can be made consistent with the observations. Here we demonstrate a stronger result: models with transient acceleration can mimic Λ CDM at all times up to the present. In our model, $w = -1$ initially, since the field begins with $\dot{\phi} = 0$. As the field begins to roll down the potential, w increases away from -1 . In Fig. 2 we have mapped out the regions in parameter space for which $-1 < w < -0.95$ at all times up to the present (which we take to correspond to $\Omega_\phi = 0.7$); this is the region below the green (dashed) curve. The region below the red (dotted) curve defines the set of parameters for which $-1 < w < -0.9$ at all times up to the present. Thus, the region between the black curve and the green curve is essentially indistinguishable from Λ CDM on the basis of current observations, and yet it results in an evolution in which the current accelerated phase of the expansion will eventually come to an end.

2.2.2 Other inflection point models

Although the simplest inflection point potential is the cubic potential considered in the previous section, more general models of the form

$$\begin{aligned} V(\phi) &= V_0 + V_n \phi^n, \quad n \text{ odd} \\ V(\phi) &= V_0 + V_n \text{sgn}(\phi) \phi^n, \quad n \text{ even} \end{aligned} \quad (44)$$

are also possible. Models of this sort were discussed briefly in Ref. [52] in the context of inflation.

Consider first the case $n = 2$. The evolution of a quintessence field in a potential of the form

$$V(\phi) = V_0 + V_2 \phi^2, \quad (45)$$

was analyzed in Ref. [43], based on the results of Ref. [42], for a universe containing both matter and a scalar field, in the limit where

$$\frac{1}{V} \frac{dV}{d\phi} \ll 1. \quad (46)$$

In this limit, two behaviors are possible, based on the value of $(1/V)(d^2V/d\phi^2)$ at the minimum of the potential. When $(1/V)(d^2V/d\phi^2) < 3/4$ at the minimum of the potential, the scalar field asymptotically approaches 0, while for $(1/V)(d^2V/d\phi^2) > 3/4$, the field oscillates around the minimum [43].

The $n = 2$ case of Eq. (44) is identical to Eq. (45) for $\phi > 0$, so the results of Ref. [43] carry over directly to the inflection point case: for $(1/V)(d^2V/d\phi^2) < 3/4$ the scalar field will

never cross the inflection point, while for $(1/V)(d^2V/d\phi^2) > 3/4$ the field will evolve across the inflection point and the accelerated expansion will be transient.

In terms of the parameters V_0 and V_2 in Eq. (44), the condition for evolution through the inflection point becomes

$$\frac{V_2}{V_0} > \frac{3}{8}. \quad (47)$$

Conversely, when Eq. (47) is not satisfied, the scalar field evolves to $\phi = 0$ asymptotically. The “slow-roll” condition for the results of Ref. [43] to be valid (Eq. (46)) will be satisfied for

$$\frac{2V_2\phi}{V_0} \ll 1. \quad (48)$$

Note, however, that as $\phi \rightarrow 0$, Eq. (48) is always eventually satisfied, so Eq. (47) provides the correct condition for evolution through the inflection point for arbitrary initial values of ϕ ; we have verified this result numerically.

Thus, the evolution of ϕ for the $n = 2$ case of Eq. (44) qualitatively resembles the results shown in Fig. 2 for the cubic inflection point potential when the latter has large ϕ_i , albeit with a different critical value for V_n/V_0 . Thus, while the $n = 2$ case is somewhat unnatural, it does provide insight into the qualitative behavior of the more interesting $n = 3$ case.

However, the behavior of these two models is quite different for small ϕ_i . In this case, transition through the inflection point for $n = 3$ requires increasingly large values of V_3/V_0 as $\phi_i \rightarrow 0$, while for $n = 2$ the critical value for V_2/V_0 remains constant for all ϕ_i .

Now consider larger values of n . The evolution of scalar field potentials of the form

$$V(\phi) = V_n\phi^n \quad (49)$$

for the case of a matter-dominated expansion was previously examined in Ref. [38]: for $n > 6$, the field evolves smoothly to $\phi \rightarrow 0$ as $t \rightarrow \infty$. (See also the discussion in Ref. [71].) In the case considered here, we have an additional contribution to H in Eq. (33): the contribution of the scalar field energy density, which now also includes the additional constant term, V_0 , in the scalar field potential. However, this additional contribution to the friction term in Eq. (33) can only serve to decrease $\dot{\phi}$ as the scalar field rolls toward the inflection point, making it more difficult for the field to reach $\phi = 0$. Thus, we can conclude from the results of Ref. [38] that inflection point potentials of the form given in Eq. (44) with $n > 6$ never transition through the inflection point.

The cases $n = 4, 5, 6$ are neither as interesting as $n = 3$ nor as amenable to analytic solution as $n = 2$ or $n > 6$, so we will not discuss them in detail here. However, numerical integration indicates that, like the $n = 3$ case, they can yield either evolution of the scalar field through the inflection point, or attraction to the inflection point, depending on the model parameters.

The simple cubic inflection point model given by Eq. (38) can also be generalized by adding linear and quadratic terms as in Eq. (39). Note that the quadratic term can be eliminated by a suitable translation of ϕ , and we can set the corresponding (new) value of ϕ_0 to zero as in the previous section, to yield

$$V(\phi) = V_0 + V_1\phi + V_3\phi^3. \quad (50)$$

The evolution of ϕ will then depend on the sign of V_1 . For $V_1 > 0$, the potential has no local minima, and the field will always transition through the inflection point at $\phi = 0$. However, for

sufficiently small V_1 , one can still have a model arbitrarily close to Λ CDM. Thus, in this variant of inflection point quintessence, the accelerated expansion of the universe is always a transient phenomenon.

On the other hand, if $V_1 < 0$, the potential develops a local minimum at $\phi = \sqrt{-V_1/3V_3}$ and a local maximum at $\phi = -\sqrt{-V_1/3V_3}$. Depending on the parameter values and initial conditions for ϕ , it is possible for the field to transition through the local maximum, so that the accelerated expansion of the universe is transient, or to get trapped in the local minimum, producing eternal acceleration. This behavior resembles the evolution of the scalar field in the Albrecht–Skordis model [72], in which the potential is given by the product of an exponential and a polynomial, producing local minima in $V(\phi)$. In the Albrecht–Skordis model, the accelerated expansion of the universe can be either permanent or transient, depending on the model parameters [61].

2.3 Conclusions

Inflection point quintessence represents an interesting new model for the dark energy that drives the accelerated expansion of the universe. Even the simplest form of this model, with the potential given by Eq. (38) and the scalar field initially at rest, displays a variety of intriguing behaviors. For large initial values of ϕ , the asymptotic behavior of ϕ becomes independent of ϕ_i and depends only on V_3/V_0 , while for small ϕ_i , the behavior depends on both V_3/V_0 and ϕ_i . In either case, it is possible to have asymptotic evolution for which $\phi \rightarrow 0$, and the universe undergoes eternal de Sitter expansion, or, conversely, for ϕ to transition through the inflection point, leading to transient acceleration.

It is interesting to note that this potential can yield an attractor at $\phi = 0$ despite the fact that $V(\phi)$ has an inflection point, rather than a local minimum, at $\phi = 0$. On the other hand, it is possible to construct models very close to Λ CDM today which nonetheless evolve away from accelerated expansion in the future.

Inflection point quintessence shows, within the context of a very simple model, that current data may never be sufficient to determine whether the universe will accelerate forever or simply pass through a transient period of acceleration. While we have not explored in similar detail the more general inflection point models given by Eq. (50), these models, too, can give rise to either eternal de Sitter expansion or transient acceleration, but in this case the asymptotic behavior depends strongly on the sign of the linear term.

CHAPTER 3

A MODIFIED EXPONENTIAL POTENTIAL FOR QUINTESSENCE

3.1 Introduction

One of the earliest quintessence models to be investigated is the exponential potential,

$$V(\phi) = V_0 e^{-\lambda\phi}. \quad (51)$$

(We work in units for which $\hbar = c = 8\pi G = 1$ throughout.) This potential arises naturally in the context of Kaluza–Klein theories, as well as in a variety of supergravity models (see, e.g., Ref. [73] for a discussion). It was first explored in connection with inflation, where it produces a power-law expansion [74–76].

Later this potential was examined as a possible model for quintessence [36, 73, 77, 78]. The exponential potential has the interesting property of generating tracking solutions, i.e., for an appropriate choice of λ , the quintessence field evolves like radiation during the radiation-dominated era, and like matter in the matter-dominated era. This held the promise of resolving the coincidence problem, since the quintessence field can evolve as a relatively large and constant fraction of the matter density up to the present. However, it was soon realized that such models cannot generate the observed accelerated expansion of the universe at late times, and they were largely abandoned.

Later, Barreiro et al. [79], attempted to resurrect the exponential quintessence model by introducing a scalar field with a potential given by a sum of exponentials. Here we investigate a simpler mechanism to allow the exponential potential to serve as a quintessence field: an exponential potential with a nonzero offset in the potential, so that:

$$V(\phi) = V_0 (1 + e^{-\lambda\phi}). \quad (52)$$

In the next section, we explore the evolution of this scalar field, and show that it gives behavior consistent with an accelerating universe. In Sec. 3.3, we examine observational constraints on this model. Our conclusions are discussed in Sec. 3.4.

3.2 Evolution of the scalar field

The equation of motion for a scalar field ϕ in the expanding universe is

$$\ddot{\phi} + 3H\dot{\phi} + \frac{dV}{d\phi} = 0, \quad (53)$$

where the dot indicates the derivative with respect to time, and H is the Hubble parameter, given by

$$H^2 = \left(\frac{\dot{a}}{a} \right)^2 = \frac{\rho}{3}, \quad (54)$$

where ρ is the total density, and we assume throughout a spatially flat universe. The scalar field energy density and pressure are given, respectively, by

$$\rho_\phi = \frac{1}{2} \dot{\phi}^2 + V(\phi) \quad (55)$$

and

$$p_\phi = \frac{1}{2} \dot{\phi}^2 - V(\phi), \quad (56)$$

and the equation of state parameter, w , is given by Eq. (13).

In the standard cosmological model (without quintessence), the density in Eq. (54) is dominated at early times by radiation, with a density scaling as

$$\rho_R = \rho_{R0} a^{-4}, \quad (57)$$

while at late times it is dominated by matter, with a density given by

$$\rho_M = \rho_{M0} a^{-3}. \quad (58)$$

In general, if the universe is dominated by a component with equation of state parameter, w , then the density will scale as

$$\rho(a) = \rho_0 a^{-3(1+w)}. \quad (59)$$

We can therefore define a “background” equation of state parameter, w_b , which is given by

$w_b = 1/3$ during the radiation-dominated era, and $w_b = 0$ during the matter-dominated era.

Now consider the evolution of ϕ for the exponential potential given by Eq. (51). For this case, Eq. (53) has no analytic solution. However, it is possible to show that there is an “attractor” toward which the solution evolves. For

$$\lambda^2 > 3(1 + w_b), \quad (60)$$

this attractor is characterized by an equation of state

$$w_\phi = w_b, \quad (61)$$

and a density, relative to the total density, of

$$\Omega_\phi \equiv \frac{\rho_\phi}{\rho_\phi + \rho_b} = \frac{3(1 + w_b)}{\lambda^2}, \quad (62)$$

where ρ_b represents the background energy density. (See Refs. [73] and [78] for the derivation of these results). Thus, during the radiation-dominated era, the scalar field evolves like radiation, with $w_b = 1/3$ and $\Omega_\phi = 4/\lambda^2$, whereas during the matter-dominated era it evolves like matter, with $w_b = 0$ and $\Omega_\phi = 3/\lambda^2$. When Eq. (60) is not satisfied, the attractor is instead inflationary: the scalar field comes to dominate and $w_\phi \rightarrow -1$.

Clearly, this model cannot account for the dark energy, since observations indicate that $w_\phi \approx -1$ at the present [9–11, 32–35]. Therefore, we modify the potential as in Eq. (52). In this model, V_0 must be fixed to give the correct present–day dark energy density, leaving only a single free parameter, λ .

Using the results of Refs. [73–78], it is possible to derive an approximate analytic prediction of the evolution of ϕ in this case. At early times, the exponential term in the potential dominates, so we have tracking behavior, with the field evolving like radiation during the radiation–dominated era, and like matter during the matter–dominated era. At late times, the V_0 term begins to become important. To estimate the evolution in this case, we can represent the scalar field as the sum of a constant–density part (with potential V_0) and a new field, $\tilde{\phi}$, which evolves in the pure exponential potential given by Eq. (51). In essence, our model is identical to a quintessence field with a purely exponential potential evolving in a Λ CDM background.

Thus, at late times, $\tilde{\phi}$ tracks w_b as w_b evolves from 0 to -1 . However, note that at the same time Eq. (62) implies that $\Omega_{\tilde{\phi}} \rightarrow 0$ as $w_b \rightarrow -1$. The result is that ρ_ϕ scales first like matter, and then like a cosmological constant, but the evolution is not identical to simply adding an additional dark matter component at early times and a cosmological constant at late times. In our model, the dark energy density decays slowly toward a constant at late times.

To see the exact evolution, we have numerically integrated Eq. (53) with the potential given by Eq. (52) for the sample cases $\lambda = 10, 13$ and 15 . Since we are interested in the late–time evolution relevant for quintessence, we do not include the radiation component. We allow the evolution to attain the tracker solution evolution at early times, and then integrate forward to the present day, which we define to be the scale factor at which $\Omega_\phi = 0.7$.

Fig. 3 shows the evolution of w_ϕ as a function of the scale factor a , where $a=1$ at the present. Note that our solution is incorrect during the radiation-dominated era ($a \lesssim 10^{-3}$), but we extend the curves all the way back to $a=0$ for simplicity. As expected, the equation of state parameter evolves smoothly from $w_\phi = 0$ to $w_\phi = -1$ at the present, but the details of the evolution depend on the actual value of λ .

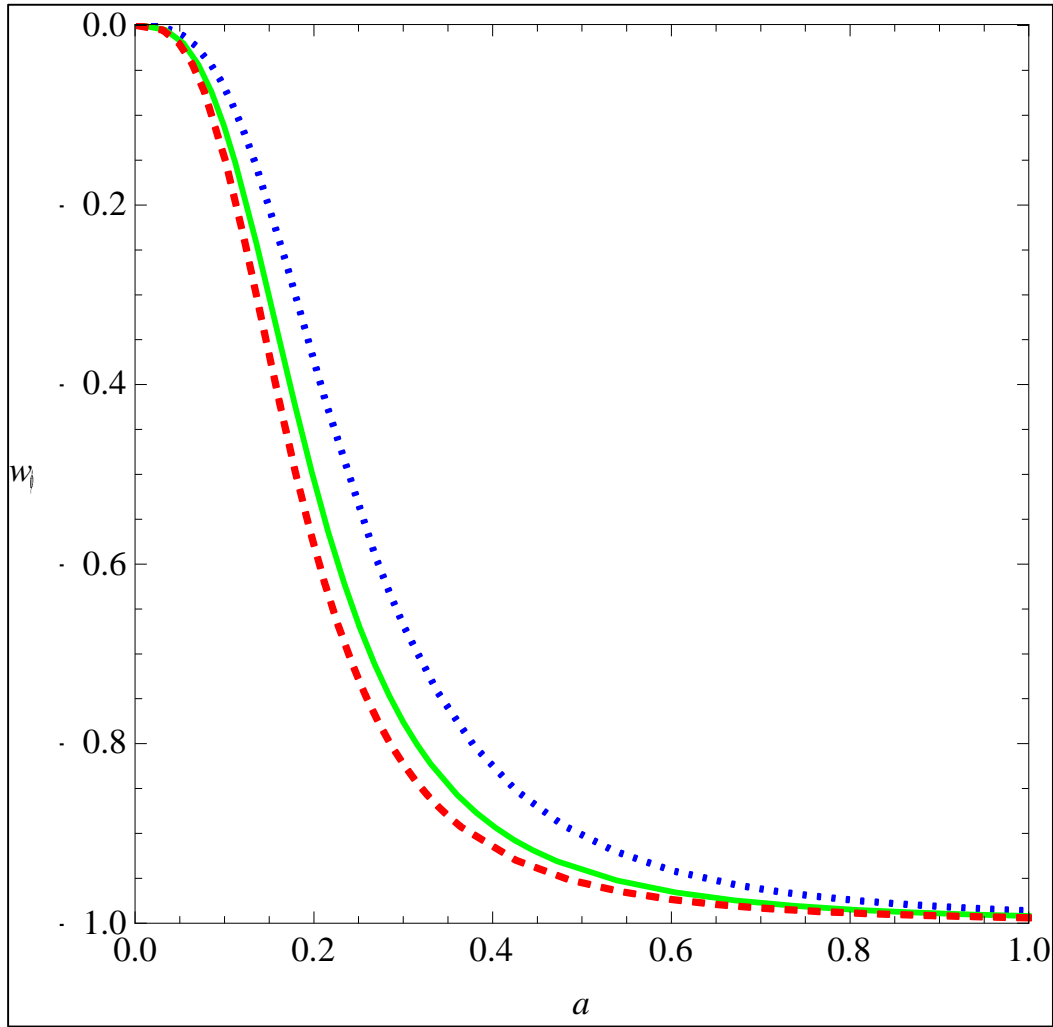


Fig. 3. The evolution of the scalar field equation of state w_ϕ as a function of the scale factor a , where $a=1$ at the present. Blue (dotted) curve is for $\lambda=10$; green (solid) curve is for $\lambda=13$; red (dashed) curve is for $\lambda=15$.

In Fig. 4, we show the density parameter for the quintessence field, Ω_ϕ , as a function of a . At small a , the curve is nearly horizontal, as Ω_ϕ is nearly constant and equal to its tracker value, while at late times the curve evolves toward its present-day value of $\Omega_\phi \approx 0.7$.

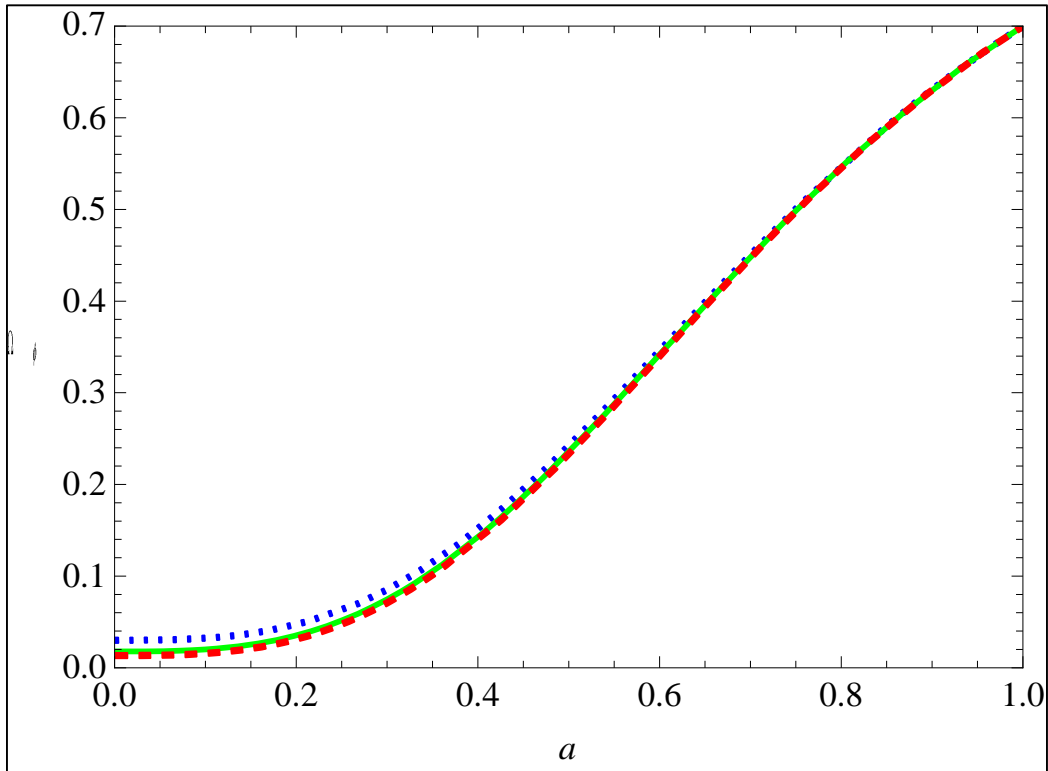


Fig. 4. The evolution of the scalar field energy density parameter, Ω_ϕ , as a function of the scale factor a , where $a=1$ at the present. Blue (dotted) curve is for $\lambda=10$; green (solid) curve is for $\lambda=13$; red (dashed) curve is for $\lambda=15$.

3.3 Observational constraints

Observational data place strong constraints on models with significant early dark energy, like the one presented here. Prior to precision Cosmic Microwave Background (CMB) experiments, the best limits came from upper bounds on the energy density during big-bang

nucleosynthesis (BBN). However, these limits have been superseded by constraints from the CMB, so the CMB constraints are the limits we will use here.

We first note that while the density of the quintessence field evolves as radiation during the radiation-dominated era, and as matter during the matter-dominated era, its clustering behavior is not identical to either radiation or matter during these epochs. The reason is that scalar fields are characterized by a sound speed of $c_s^2 = 1$. In contrast, cold dark matter has $c_s^2 = 0$ and radiation has $c_s^2 = 1/3$. This difference is most noticeable during the matter-dominated era. Because of its large sound speed, the scalar field does not cluster, so even a small admixture of the scalar field can produce a distinct imprint on the CMB.

CMB limits on additional energy density have been discussed, e.g., by Calabrese et al. [80], Samsing et al. [81], and Hojjati et al. [82]. The most useful limits for our purposes come from Hojjati et al., who provide upper bounds on additional energy density as a function of both redshift and sound speed, using data from Planck and the Nine-Year Wilkinson Microwave Anisotropy Probe (WMAP9) observations. They parametrize the change in the expansion rate from an additional component in terms of a parameter δ , defined by

$$H(a)^2 = \frac{\rho_{standard}(a)}{3} [1 + \delta(a)], \quad (63)$$

where $\rho_{standard}$ is the energy density in the standard Λ CDM model.

In either the matter-dominated or radiation-dominated eras, the relation between Ω_ϕ in our model and δ in Ref. [82] is given by

$$\Omega_\phi = \frac{\delta}{1 + \delta}, \quad (64)$$

so that

$$\lambda = \sqrt{k \left(\frac{1}{\delta} + 1 \right)}, \quad (65)$$

where $k \equiv 3(1 + w_b)$. Therefore, $k = 3$ during the matter-dominated era, and 4 during the radiation-dominated era.

For $c_s^2 = 1$, the constraints on δ as a function of redshift from Ref. [82] are

$$\delta < 0.036 \quad a = 10^{-4.5}, \quad (66)$$

$$\delta < 0.050 \quad a = 10^{-3.8}, \quad (67)$$

$$\delta < 0.160 \quad a = 10^{-3.4}, \quad (68)$$

$$\delta < 0.095 \quad a = 10^{-3.0}, \quad (69)$$

$$\delta < 0.018 \quad a = 10^{-1.4}. \quad (70)$$

The tightest constraints on δ occur at the lowest redshift z ($z = 1/a - 1$) examined in Ref. [82], namely at $a = 10^{-1.4}$, for which $\delta < 0.018$. This contrasts sharply from the $c_s^2 = 0$ case, for which there is essentially no constraint during the matter-dominated era (since the additional component in this case simply gets absorbed into the definition from the cold dark matter density), and the tightest constraints come from the radiation-dominated era. Taking $\delta < 0.018$ in Eq. (65) gives $\lambda > 13$. Thus, the regions in parameter space above the solid curves in Figs. 3 and 4 are ruled out. In terms of Ω_ϕ , this bound translates into:

$$\Omega_\phi < 0.018, \text{ matter-dominated era} \quad (71)$$

$$\Omega_\phi < 0.024, \text{ radiation-dominated era} \quad (72)$$

While the quintessence field does not behave exactly like extra radiation during the radiation-dominated era (because it has $c_s^2 = 1$ rather than $1/3$) it is nonetheless instructive to see what energy density our limit corresponds to in the radiation era in terms of the effective

number of additional neutrinos. In the radiation-dominated era, the number of additional neutrinos is related to Ω_ϕ as [80]

$$\Delta N_{eff} = 7.44 \frac{\Omega_\phi}{1 - \Omega_\phi}. \quad (73)$$

Then our limit in Eq. (72) corresponds to $\Delta N_{eff} < 0.18$.

3.4 Discussion

It is clear from Fig. 3 that our modified exponential potential can provide a plausible model for the accelerated expansion of the universe, with an evolution for w_ϕ that differs from that of Λ CDM. However, that evolution diverges only slightly from standard Λ CDM's. For the observational bound $\lambda > 13$, the value of the equation of state parameter at a redshift of $z = 1$ ($a = 0.5$) is $w_\phi \lesssim -0.95$, which then declines toward $w_\phi \approx -1$ at present. In the terminology of Caldwell and Linder [83], these are “freezing” models.

While it will be very difficult to distinguish these models from Λ CDM using, e.g., supernova determinations of the cosmic equation of state, these models, rather unusually for quintessence, will actually be more strongly constrained (or confirmed) with improved CMB data. As noted in the previous section, a large region of parameter space is already ruled out by the Planck and WMAP9 data, so additional CMB data will either drive the allowed value of λ to such a large number that the model becomes essentially indistinguishable from Λ CDM, or else show anomalies due to additional energy density at early times.

Now consider the issue of the coincidence problem, which was one of the original motivations for introducing quintessence with an exponential potential. Does our modified model provide an amelioration for the cosmic coincidence? The coincidence problem can be

stated in two different ways. One is the fact that the dark energy density is of the same order of magnitude as the matter density today: $\rho_M \sim \rho_{DE}$. This is odd because the matter density scales as a^{-3} , while a dark energy component derived from, e.g., a cosmological constant, has a constant energy density. Thus, we expect $\rho_M \gg \rho_{DE}$ at early times, and $\rho_M \ll \rho_{DE}$ in the far future, therefore it is peculiar to find that $\rho_M \sim \rho_{DE}$ today. This leads to a second statement of the coincidence problem: the “why now?” issue. Why do we happen to live at a special epoch when the dark energy density is beginning to dominate the expansion?

Our model does, to some extent, ameliorate the coincidence problem when it is expressed in terms of energy densities. At early times, the quintessence density tracks the radiation and matter densities, so there is a long period of time in the universe for which these quantities are not separated by many orders of magnitude. (Although the bounds quoted in the previous section imply $\rho_{DE} \lesssim 0.02\rho_{M,R}$.) On the other hand, the model does nothing to answer the question of “why now”? The model parameters must still be tuned so that the V_0 term in Eq. (52) begins to dominate the $V_0 e^{-\lambda\phi}$ term at around the present day. Perhaps the most interesting result is that this model shows that these two ways of expressing the coincidence problem may not be, as is usually assumed, entirely equivalent. It is possible to construct a model (i.e., this one) for which the densities of the dark energy and matter are not widely separated over much of the early universe, but which still retains the need for us to live in a “special” epoch, when the acceleration is just beginning.

REFERENCES

- [1] E.J. Copeland, M. Sami, and S. Tsujikawa, *Int. J. Mod. Phys. D* **15**, 1753 (2006).
- [2] D.N. Spergel *et al.*, *Astrophys. J. Suppl.* **170**, 377 (2007).
- [3] S. Perlmutter *et al.*, *Astrophys. J.* **517**, 565 (1999).
- [4] S. Weinberg, *Rev. Mod. Phys.* **61**, 1 (1989).
- [5] S. Dodelson, *Modern Cosmology* (2003).
- [6] A. Liddle, *An Introduction to Modern Cosmology* (1999).
- [7] H.-Y. Chang and R.J. Scherrer, *Phys. Rev. D* **86**, 027303 (2012).
- [8] H.-Y. Chang and R.J. Scherrer, *Phys. Rev. D* **88**, 083003 (2013).
- [9] M. Kowalski *et al.*, *Astrophys. J.* **686**, 749 (2008).
- [10] L. Perivolaropoulos and A. Shafieloo, *Phys. Rev. D* **79**, 123502 (2009).
- [11] M. Hicken *et al.*, *Astrophys. J.* **700**, 1097 (2009).
- [12] E. Komatsu *et al.*, *Astrophys. J. Suppl.* **180**, 330 (2009).
- [13] W.M. Wood-Vasey *et al.*, *Astrophys. J.* **666**, 694 (2007).
- [14] T.M. Davis *et al.*, *Astrophys. J.* **666**, 716 (2007).
- [15] C. Armendariz-Picon, V. Mukhanov and P.J. Steinhardt, *Phys. Rev. Lett.* **85**, 4438 (2000).
- [16] S. Dodelson, M. Kaplinghat and E. Stewart, *Phys. Rev. Lett.* **85**, 5276 (2000).
- [17] B. Feng, M.X. Li, Y.S. Piao, X.M. Zhang, *Phys. Lett. B* **634**, 101 (2006).
- [18] K. Griest, *Phys. Rev. D* **66**, 123501 (2002).
- [19] G. Huey and B.D. Wandelt, *Phys. Rev. D* **74**, 023519 (2006).
- [20] L.P. Chimento, A.S. Jakubi, D. Pavon and W. Zimdahl, *Phys. Rev. D* **67**, 083513 (2003).
- [21] J. Garriga and A. Vilenkin, *Phys. Rev. D* **67**, 043503 (2003).
- [22] R.J. Scherrer, *Phys. Rev. D* **71**, 063519 (2005).

- [23] R.R. Caldwell, Phys. Lett. B **545**, 23 (2002).
- [24] R.R. Caldwell, M. Kamionkowski and N.N. Weinberg, Phys. Rev. Lett. **91**, 071301 (2003).
- [25] A. Barreira and P.P. Avelino, Phys. Rev. D **83**, 103001 (2011).
- [26] C.H. Lineweaver and C.A. Egan, Astrophys. J. **671**, 853 (2007).
- [27] C.A. Egan and C.H. Lineweaver, Phys. Rev. D **78**, 083528 (2008).
- [28] C. Ilie, T. Biswas and K. Freese, Phys. Rev. D **80**, 103521 (2009).
- [29] P. Creminelli, M.A. Luty, A. Nicolis, and L. Senatore, JHEP **0612**, 080 (2006).
- [30] H.H. Xiong, Y.F. Cai, T. Qiu, Y.S. Piao, and X.M. Zhang, Phys. Lett. B **666**, 212 (2008).
- [31] J. Kujat, R.J. Scherrer, and A.A. Sen, Phys. Rev. D **74**, 083501 (2006).
- [32] R.A. Knop *et al.*, Ap.J. **598**, 102 (2003).
- [33] A.G. Riess *et al.*, Ap.J. **607**, 665 (2004).
- [34] G. Hinshaw *et al.*, [arXiv:1212.5226], (2013).
- [35] P.A.R. Ade *et al.*, [arXiv:1303.5076], (2014).
- [36] B. Ratra and P.J.E. Peebles, Phys. Rev. D **37**, 3406 (1988).
- [37] R.R. Caldwell, R. Dave and P.J. Steinhardt, Phys. Rev. Lett. **80**, 1582 (1998).
- [38] A.R. Liddle and R.J. Scherrer, Phys. Rev. D **59**, 023509 (1999).
- [39] P.J. Steinhardt, L.M. Wang and I. Zlatev, Phys. Rev. D **59**, 123504 (1999).
- [40] R.J. Scherrer and A.A. Sen, Phys. Rev. D **77**, 083515 (2008).
- [41] S. Dutta and R.J. Scherrer, Phys. Lett. B **704**, 265 (2011).
- [42] S. Dutta and R.J. Scherrer, Phys. Rev. D **78**, 123525 (2008).
- [43] S. Dutta, E.N. Saridakis and R.J. Scherrer, Phys. Rev. D **79**, 103005 (2009).
- [44] R. Allahverdi, K. Enqvist, J. Garcia-Bellido, and A. Mazumdar, Phys. Rev. Lett. **97**, 191304 (2006).

- [45] R. Allahverdi, K. Enqvist, J. Garcia–Bellido, A. Jokinen, and A. Mazumdar, JCAP **0706**, 019 (2007).
- [46] R. Allahverdi, A. Kusenko, and A. Mazumdar, JCAP **0707**, 018 (2007).
- [47] D. Baumann, A. Dymarsky, I.R. Klebanov, L. McAllister, and P.J. Steinhardt, Phys. Rev. Lett. **99**, 141601 (2007).
- [48] S. Panda, M. Sami, and S. Tsujikawa, Phys. Rev. D **76**, 103512 (2007).
- [49] N. Itzhaki and E.D. Kovetz, JHEP **0710**, 054 (2007).
- [50] A. Krause and E. Pajer, JCAP **0807**, 023 (2008).
- [51] R. Allahverdi, B. Dutta, and A. Mazumdar, Phys. Rev. D **78**, 063507 (2008).
- [52] N. Itzhaki and E.D. Kovetz, Class. Quant. Grav. **26**, 135007 (2009).
- [53] K. Enqvist, A. Mazumdar, and P. Stephens, JCAP **1006**, 020 (2010).
- [54] S. Hotchkiss, A. Mazumdar, and S. Nadathur, JCAP **1106**, 002 (2011).
- [55] A. Chatterjee and A. Mazumdar, JCAP **1109**, 009 (2011).
- [56] S. Downes, B. Dutta, and K. Sinha, Phys. Rev. D **86**, 103509 (2012).
- [57] S. Downes and B. Dutta, Phys. Rev. D **87**, 183518 (2012).
- [58] S. Choudhury, A. Mazumdar, and S. Pal, JCAP **07**, 041 (2013).
- [59] S. Hellerman, N. Kaloper, and L. Susskind, JHEP **0106**, 3 (2001).
- [60] W. Fischler, A. Kashani–Poor, R. McNees, and S. Paban, JHEP **0107**, 003 (2001).
- [61] J. Barrow, R. Bean, and J. Magueijo, Mon. Not. R. Astr. Soc. **316**, L41 (2000).
- [62] J.M. Cline, JHEP **0108**, 35 (2001).
- [63] R. Cardenas, T. Gonzalez, Y. Leiva, O. Martin, and I. Quiros, Phys. Rev. D **67**, 083501 (2003).
- [64] V. Sahni and Y. Shtanov, JCAP **11**, 14 (2003).

- [65] D. Blais and D. Polarski, Phys. Rev. D **70**, 084008 (2004).
- [66] N. Bilic, G.B. Tupper, and R.D. Viollier, JCAP **0510**, 003 (2005).
- [67] A.A. Sen and R.J. Scherrer, Phys. Rev. D **72**, 063511 (2005).
- [68] F.C. Carvalho, J.S. Alcaniz, J.A.S. Lima, and R. Silva, Phys. Rev. Lett. **97**, 081301 (2006).
- [69] M.C. Bento, R. Gonzalez Felipe, and N.M.C. Santos, Phys. Rev. D **77**, 123512 (2008).
- [70] W.P. Cui, Y. Zhang, and Z.W. Fu, [arXiv:1303.2315], (2013).
- [71] S. Dutta and R.J. Scherrer, Phys. Rev. D **78**, 083512 (2008).
- [72] A. Albrecht and C. Skordis, Phys. Rev. Lett. **84**, 2076 (2000).
- [73] P.G. Ferreira and M. Joyce, Phys. Rev. D **58**, 023503 (1998).
- [74] F. Lucchin and S. Matarrese, Phys. Rev. D **32**, 1316 (1985).
- [75] J.J. Halliwell, Phys. Lett. B **185**, 341 (1987).
- [76] B. Burd and J.D. Barrow, Nucl. Phys. B **308**, 929 (1988).
- [77] C. Wetterich, Nucl. Phys. B **302**, 668 (1988).
- [78] E.J. Copeland, A.R. Liddle and D. Wands, Phys. Rev. D **57**, 4686 (1998).
- [79] T. Barreiro, E.J. Copeland, and N.J. Nunes, Phys. Rev. D **62**, 123503 (2000).
- [80] E. Calabrese, D. Huterer, E.V. Linder, A. Melchiorri, and L. Pagano, Phys. Rev. D **83**, 123504 (2011).
- [81] J. Samsing, E.V. Linder, and T.L. Smith, Phys. Rev. D **86**, 123054 (2012).
- [82] A. Hojjati, E.V. Linder and J. Samsing, Phys. Rev. Lett. **111**, 041301 (2013).
- [83] R.R. Caldwell and E.V. Linder, Phys. Rev. Lett. **95**, 141301 (2005).